PHYSICAL REVIEW B **94**, 100403(R) (2016)

Bose glass behavior in $(Yb_{1-x}Lu_x)_4As_3$ representing randomly diluted quantum spin-$\frac{1}{2}$ chains

G. Kamieniarz
Faculty of Physics, A. Mickiewicz University, ul. Umultowska 85, 61-614 Poznań, Poland
and Max Planck Institute for the Physics of Complex Systems, 01187 Dresden, Germany

R. Matysiak*
Institute of Engineering and Computer Education, University of Zielona Góra, ul. prof. Z. Szafrana 4, 65-516 Zielona Góra, Poland

P. Gegenwart
Max Planck Institute for Chemical Physics of Solids, 01187 Dresden, Germany
and Experimental Physics VI, Center for Electronic Correlations and Magnetism, University of Augsburg, 86159 Augsburg, Germany

A. Ochiai
Center for Low Temperature Science, Tohoku University, Sendai 980-8578, Japan

F. Steglich
Max Planck Institute for Chemical Physics of Solids, 01187 Dresden, Germany

(Received 24 November 2015; revised manuscript received 6 September 2016; published 23 September 2016)

The site-diluted compound $(Yb_{1-x}Lu_x)_4As_3$ is a scarce realization of the linear Heisenberg antiferromagnet partitioned into finite-size segments and is an ideal model compound for studying field-dependent effects of quenched disorder in the one-dimensional antiferromagnets. It differentiates from the systems studied so far in two aspects—the type of randomness and the nature of the energy gap in the pure sample. We have measured the specific heat of single-crystal $(Yb_{1-x}Lu_x)_4As_3$ in magnetic fields up to 19.5 T. The contribution $C_\perp$ arising from the magnetic subsystem in an applied magnetic field perpendicular to the chains is determined. Compared to pure Yb_4As_3, for which $C_\perp$ indicates a gap opening, for diluted systems a nonexponential decay is found at low temperatures which is consistent with the thermodynamic scaling of the specific heat established for a Bose-glass phase.

DOI: 10.1103/PhysRevB.94.100403

An exact correspondence between a quantum antiferromagnet and a lattice Bose gas was recognized [1] much before Bose-Einstein condensation (BEC) was predicted in a three-dimensional array of antiferromagnetically coupled ladders or dimers [2–4] and was experimentally observed [5,6] in the magnetic compound $TlCuCl_3$. In spin-gap systems, apart from the superfluid and Mott insulating states, a Bose-glass state was also predicted [7]. Since this observation in $TlCuCl_3$, a search for the BEC transitions and a Bose-glass (BG) phase in magnetic materials has hastened [8,9], including also the spin-gap $S = 1$ Haldane chains [10–12] or quasi-one-dimensional systems consisting of weakly interacting chains or two-leg ladders [13,14].

In spin-gap one-dimensional antiferromagnets (AFM) the ground state is a spin singlet separated by a finite energy gap Δ from the first excited state which is a spin triplet. In the integer-spin chains the gap Δ exists for uniform systems [15], whereas in the case of the half-integer-spins, the gap may originate from the bond alternation. Then the pairs of strongly coupled spins exhibit the dimer singlet ground states which contribute to the ground state of the chain. However, the energy structure with a nonmagnetic singlet ground state is unstable for magnetic fields exceeding the critical value B_c corresponding to Δ or for a sufficient level of dilution [14].

The BG state is an unusual state of matter with no broken symmetry and no energy gap in the excitation spectrum. This feature of BG was found for interacting bosons in quenched disordered systems [9,12,14,16]. The gapless nature of the BG state is characterized in the presence of an external magnetic field by an exponential magnetization behavior [17], a finite uniform magnetic susceptibility, and a nonexponential decay of the low-temperature specific heat [9]. The thermodynamic signature which uniquely characterizes the main features of the BG and Mott glass phases is a stretched exponential behavior of the specific heat [9] given by the expression

$$C(T) = A(k_BT/J)^{-5/4}\exp(-\gamma(k_BT/J)^{-1/2}), \qquad (1)$$

where the parameters A and γ depend both on a concentration of impurities and on magnetic field, and J represents a leading coupling constant. The unconventional magnetization and specific heat behavior of the BG state is elucidated by a local-gap model [9,17,18], considering the lowest order finite-size scaling of the emerging energy gaps.

In the scenarios described so far, the spin gap is formed by the special *couplings* present in the quasi-one-dimensional (1d) compounds. For the integer spin $S = 1Ni^{2+}$-based compound [9], the strong easy plane anisotropy ($D/J \gg 1$) is needed, whereas for the half-integer-spin compound with two-leg ladder structures embedded, strong rung-oriented and weak leg-oriented interactions are prerequisite [13,14] to get a pseudo-$S = 1$ Haldane chain representation. The role of the

*r.matysiak@iibnp.uz.zgora.pl

 ©2016 American Physical Society

applied magnetic field is to close the spin gap and to create a finite density of bosons forming a magnetic BEC both in the pure and the doped compound [9].

However, the spin gap can also be induced by the transverse magnetic field applied in antiferromagnetic spin-1/2 chains with a Dzyaloshinskii-Moriya (DM) interaction [19–21]. A good example of such a system is Yb_4As_3 [22]. Upon dilution of Yb_4As_3 by the lutetium ions Lu^{+3}, the magnetic Yb^{3+} is substituted by the chemically identical nonmagnetic Lu^{3+}, and the charge ordering in the site-diluted $(Yb_{1-x}Lu_x)_4As_3$ is retained for $x \leqslant 0.06$ [23]. The nonmagnetic impurities are randomly distributed, giving rise to a statistical partitioning of the spin chains into even and odd-numbered segments with the gapped singlet-triplet and spin-1/2 doublet ground states, respectively [18,24]. They result in a strong reduction of *zero-field* specific heat [25] in the diluted Yb_4As_3. Moreover, the temperature dependence of the specific heat fulfills [25] the scaling law predicted for segmented Heisenberg spin chains [18] which is identical to Eq. (1) characterizing the BG state.

In this Rapid Communication we aim at showing that the title compound $(Yb_{1-x}Lu_x)_4As_3$ provides a type of the BG system under quenched doping by the nonmagnetic impurities and subject to the transverse field. We argue that we observe this BG behavior because: (a) the nonexponential decay of the low-temperature specific heat is demonstrated both in the pure sample ($x = 0\%$) and in the site-diluted samples ($x = 1\%$, $x = 3\%$) if the applied field is absent; (b) in the presence of magnetic field B with a perpendicular component, the exponential decay occurs in the pure system only, while it becomes nonexponential in the diluted systems; (c) in the latter case the stretched exponential behavior (1) of the specific heat characterizing the BG phase is validated.

The diluted Yb_4As_3 is very suitable for observation of the BG phase in quantum magnets. The diamagnetic dopands Lu^{3+} create site-diluted chains with missing adjacent bonds. The resulting system is a simple collection of finite linear segments. Its analysis is void of further approximations, in contrast to a more complex physics of the systems with randomized bonds realized so far by a bromine doping [9] which affects locally the values of couplings and anisotropy parameters and proliferates their number. Consequently, the stretched exponential scaling law can be checked unambiguously because interactions in $(Yb_{1-x}Lu_x)_4As_3$ still depend on *a single* coupling constant J, and all the model parameters are fixed.

We have performed field-dependent measurements on the single-crystal sample $(Yb_{1-x}Lu_x)_4As_3$ with $x = 1\%$ or $x = 3\%$. Both the samples and equipment were the same as those in our previous study [25]. The magnetic specific heat C_m was obtained from the measured specific heat C_{exp} by subtracting the lattice contribution C_{ph} estimated earlier [26], and assuming that the phonon part is unaffected by the field applied and the doping [see Fig. 1 in Ref. [25] and Figs. S1–S4 in the Supplemental Material (SM) [27]]. The heat capacity has been measured with error below 10%. The error is largest at the lowest T and highest field.

The magnetic field has always been applied along one of the cubic [111] directions for each studied single crystal. The charge ordering transition selects one space diagonal as the spin chain direction and results in a polydomain state

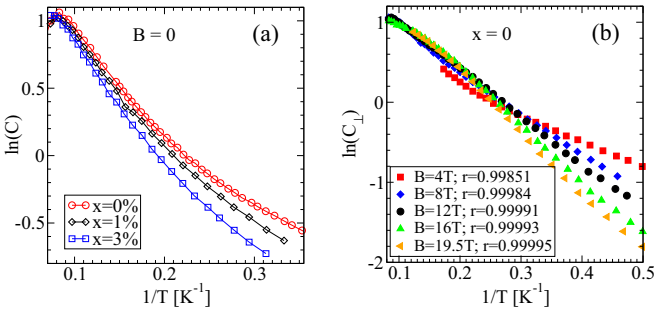

FIG. 1. (a) Molar zero-field magnetic specific heat of the pure and doped samples plotted in semilogorithmic scale as a function of $1/T$. (b) The exponential dependence of $C_\perp$ as a function of $1/T$ in the low-temperature region. The corresponding Pearson correlation coefficients r are provided.

at low temperatures. Then in 1/4 of the domains the field is parallel to the magnetic chains, whereas in the remaining 3/4 of the domains, the chains will be subject to an effective perpendicular field [25,26], so that

$$C_m(T,B) = 0.75C_\perp(T,B_{eff}) + 0.25C_\parallel(T,B), \qquad (2)$$

where $B_{eff} = B\sin(70^\circ)$ and $C_\perp = C_\parallel$ in the limit $B = 0$. Here $C_\parallel$ and $C_\perp$ denote the magnetic heat capacity contributions from domains with the chains parallel and perpendicular to the applied field, respectively.

Following the consensus that the chains are well isolated and the XXZ anisotropy between the adjacent Yb^{3+} ions is canceled by the DM antisymmetric exchange [22,28,29], the physical system is described by the one-dimensional effective spin-1/2 model

$$\mathcal{H} = J\sum_{i=1}^{L}\mathbf{S}_i\mathbf{S}_{i+1} - g_\perp\mu_B B^x\sum_{i=1}^{L}S_i^x - g_\perp\mu_B B_s^y\sum_{i=1}^{L}(-1)^i S_i^y - g_\parallel\mu_B B^z\sum_{i=1}^{L}S_i^z, \qquad (3)$$

representing the chains pointing along the z axis, subject to the perpendicular $B_\perp$ or parallel B^z field applied in the x or z direction, respectively. The lengths L of the chains are assumed to be infinite for the pure Yb_4As_3 compound and finite for doped samples. Due to the DM interaction [28,30], the perpendicular field implies both the renormalized field $B^x = B_\perp\cos(\theta)$ in the x direction and the staggered field $B_s^y = B_\perp\sin(\theta)$ in the y direction, where θ is the corresponding phase factor.

In the model (3) all the parameters are fixed, and their values arise from the earlier magnetic studies [26,29,31]. We assume here that $J/k_B = 28$ K, $g_\perp = 1.3$, $g_\parallel = 2.9$, $\tan\theta = 0.19$. The applied field B is matched to $B_\perp = B\sin(70^\circ)$ and $B^z = B$ in our model. Its thermodynamic properties are analyzed by the quantum transfer matrix (QTM) technique [25,26,32], having checked the fast convergence of approximants and the linear finite-size scaling of the specific heat in the presence of magnetic field, similar to that illustrated in Fig. 2 in Ref. [25].

In Figs. 1(a) and 1(b) some reanalyzed results for the pure [26] Yb_4As_3 and the diluted [25] $(Yb_{1-x}Lu_x)_4As_3$ are plotted. The *zero-field* data in Fig. 1(a) demonstrates the

nonexponential dependence of the molar specific heat on $1/T$ in the low temperature region regardless of the concentration x. This feature is the manifestation of an essentially gapless energy spectrum. Even though in the diluted sample the segments with even number of magnetic sites display residual energy gaps, their values are randomly distributed, their average values are small for $x \leqslant 0.03$ so that instead the stretched exponential dependence is developed [18,25].

However, in the pure sample subject to a field perpendicular to the chains ($B_\perp \neq 0, B^z = 0$), the gap should open up and bring on an exponential decay of the specific heat. The data $C_\perp(T)$ presented in Fig. 1(b) are derived from the $C_m(T)$ results given by open symbols in Fig. 5 in Ref. [26] after subtracting according to Eq. (2) the contribution $C_\parallel$ from the domains with the chains aligned along the field which was calculated, imposing $B_\perp = 0$ in the model (3). The values $0.75C_\perp$ extracted from $C_m(T)$ are very close to the corresponding QTM estimates plotted therein. In the relevant temperature region $2.5 \leqslant T \leqslant 5$ K the phonon part $C_{ph}(T)/T$ is much smaller than the contributions from $C_\parallel(T)/T$ and $C_\perp(T)/T$ shown in Fig. 5 in Ref. [26] so that phonons do not affect the accuracy of the extracted $C_\perp$.

The expected feature for the pure Yb_4As_3 is revealed in Fig. 1(b) in the low temperature region, where the linear dependence on $1/T$ is recovered for $C_\perp$. The Pearson correlation coefficients r measuring the linear correlation between two variables are sufficiently close ($0.99851 \leqslant r \leqslant 0.99995$) to the ideal value 1. In addition, referring to Eq. (1), we have analyzed the nonexponential dependence of $C_\perp$ which leads to a deterioration of the linearity ($0.99814 \leqslant r \leqslant 0.99874$, see Fig. S1 in SM).

The molar magnetic specific heat data for the diluted $(Yb_{1-x}Lu_x)_4As_3$ are plotted in Fig. 2 and compared with the results of our numerical simulations. The raw outcome of the measurements and the phonon contribution are plotted in Figs. S2–S5 in the SM [27]. In Figs. 2(a) and 2(b) the strength of applied field $B_\perp$ is fixed, whereas in Figs. 2(c) and 2(d), the impurity concentration is kept constant. The outright agreement between experiment and theory provides compelling evidence for the high quality of the model (3) and enhances confidence in our procedure (2) which enables us to extract $C_\perp$ from C_m, having calculated $C_\parallel$. In the SM [27], the $C_\parallel$ and $C_\perp$ contributions to C_m are plotted in Figs. S6–S9, and again in the low temperature region they dominate over C_{ph} so that uncertainties in C_{ph} have negligible impact on the accuracy of the $C_\perp$ extracted.

To ascertain that the specific heat behavior characteristic for the BG system is obeyed in the presence of magnetic field, only the part $C_\perp(T)$ of the experimental specific heat shown in Fig. 2 should be considered. The relevant results are plotted in molar units in Fig. 3 and contain error bars if they exceed the size of the symbols. In panels (a) and (b) we demonstrate that deviations of the specific heat from the exponential decay are stronger than those in Fig. 1(b), yielding clearly lower values of r ($r \leqslant 0.9981$). This nonlinear dependence agrees with the gapless nature of the Bose glass which is distinguished by a nonexponential decay of the specific heat.

In panels (c) and (d) of Fig. 3 the rescaled $C_\perp$ data as a function of the variable $(k_BT/J)^{-1/2}$ are plotted and the Pearson coefficients are extracted. The pronounced linear

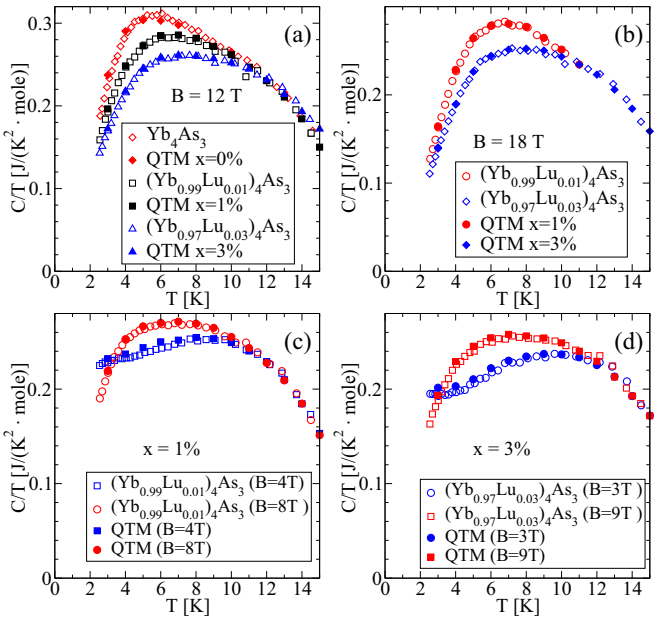

FIG. 2. Comparison between experiment and theory for the diluted samples subject to an applied field. In panels (a) and (b), the field applied is $B = 12$ T and 18 T, respectively. In panels (c) and (d), the nonmagnetic impurity concentration amounts to $x = 1\%$ and $x = 3\%$, respectively. The symbols are explained in the legend.

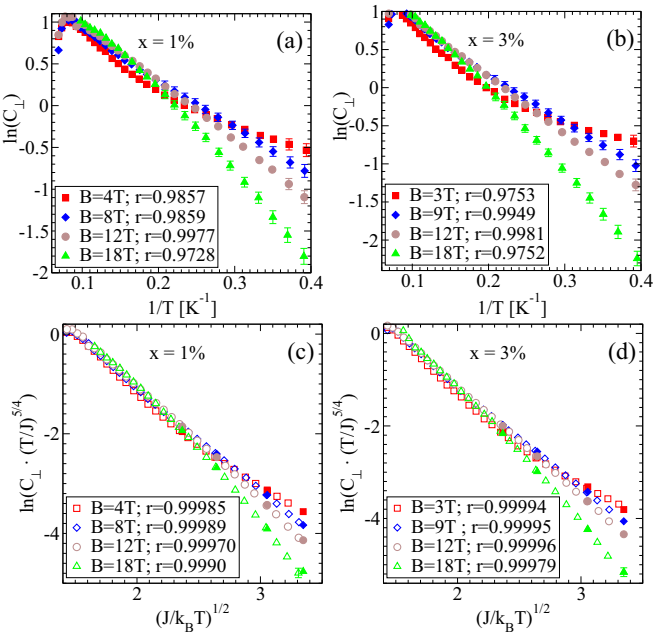

FIG. 3. The behavior of the contribution $C_\perp$ to the specific heat for the diluted $(Yb_{1-x}Lu_x)_4As_3$. In the region of low temperatures, panels (a) and (b) as well as their insets illustrate nonexponential decay of the $C_\perp(T)$ vs $1/T$. Panels (c) and (d) display the realization of the corresponding BG scaling law of $C_\perp(T)(k_BT/J)^{5/4}$ for $(J/k_BT)^{1/2} \geqslant 2.4$. The open and full symbols represent the experimental data and the QTM estimates, respectively, and the values r denote the corresponding Pearson correlation coefficients.

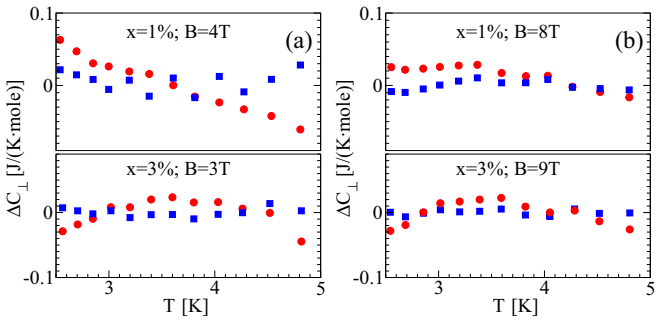

FIG. 4. The deviations of the measured $C_\perp$ data from those fitted by the exponential and the stretched exponential dependence plotted by full circles and squares, respectively. In panels (a) and (b) some representative weak and intermediate applied fields are selected. Error bars attain at most the size of the symbols and are omitted.

dependence ($0.9990 \leqslant r \leqslant 0.99996$) in the low-temperature region $T \leqslant 5.0$ K (i.e., $(k_B T/J)^{-1/2} \geqslant 2.4$) points to the stretched exponential behavior.

To check the reliability of our conclusions, we have digitalized the specific heat data plotted in Figs. 2(d) and 4 for DTN [9]. In the most favorable case $B = 0$ we found the coefficients $r = 0.99864$ for $x = 0$ and the expected exponential decay (in the region $T^{-1} > 0.96$), and $r = 0.99976$ for $x = 0.08$ and the expected stretched exponential dependence (in the interval $0.97 < T^{-1/2} < 2.5$, i.e., neglecting the extreme point lowering r). These coefficients characterizing the linear relationship are very close to the corresponding numbers calculated in our study of the Bose glass behavior in $(Yb_{1-x}Lu_x)_4As_3$.

An additional evidence for the BG scaling of the specific heat is provided by the residual values defined as the differences between the experimental data $C_\perp$ and the corresponding fits based on the exponential [Figs. 3(a) and 3(b)] and the stretched exponential [Figs. 3(c) and 3(d)] dependence. The corresponding curves in Fig. 4 are qualitatively different. Much smaller values and a random scattering of the residuals obtained for the stretched exponential decay signal the nonexponential behavior. This observation agrees with the similar outcome found for the DTN data (see Figs. S10 and S11 in the SM [27]). We note that for pure Yb_4As_3 the exponential dependence shown in Fig. 1(b) is superior to the stretched exponential counterpart as far as the Pearson coefficients and residuals are concerned (see Figs. S1, S12, and S13 in the SM).

To provide some evidence for the finite uniform susceptibility in $(Yb_{1-x}Lu_x)_4As_3$, we recall both the experimental magnetization data on DTN [Fig. 2(a) in Yu *et al.* [9]] as well as the magnetic measurements [31,33,34] performed on the pure Yb_4As_3 and the theoretical results for the model (3) obtained in some particular cases [18,35]. For the pure and doped DTN [Fig. 2(a) in Yu *et al.* [9]] the magnetization profiles nearly coincide and the latter implies a finite uniform magnetic susceptibility characteristic for the Bose glass. Likewise, the dependence of the uniform magnetization of Yb_4As_3 on the transverse magnetic field [Fig. 4 in Iwasa *et al.* [31]] implies the finite susceptibility. We can expect that the susceptibility remains finite under doping, as the local-gap model explaining the exponential suppression of magnetization in DTN [9,17] is applicable for our system [18], too. We also note that the simplified model (3) with $B^x = B^z = 0$ is akin to that describing a disordered boson chain in the limit of a large charging energy [36], where the BG phase was also established on the basis of the proper susceptibility behavior.

In conclusion, we have measured the specific heat in the site-diluted $(Yb_{1-x}Lu_x)_4As_3$ which is an ideal model compound to develop the BG behavior in the transverse magnetic field with respect to the chain direction. The relevant part $C_\perp$ of the specific heat is found to behave as predicted for a Bose-glass phase, in that it exhibits a nonexponential decay as a function of $1/T$ and obeys the proper BG scaling law.

P.G. acknowledges discussions with Andreas Honecker. This work was supported by the Polish National Science Centre Grant No. N519 579138 and it was granted access to the HPC resources in PSNC Poznań (Poland) and to the PRACE-3IP project resources (FP7 RI-312763) in CaSToRC Nicosia (Cyprus).

[1] T. Matsubara and H. Matsuda, Prog. Theor. Phys. **16**, 569 (1956).
[2] T. Giamarchi and A. M. Tsvelik, Phys. Rev. B **59**, 11398 (1999).
[3] T. M. Rice, Science **298**, 760 (2002).
[4] S. Wessel, M. Olshanii, and S. Haas, Phys. Rev. Lett. **87**, 206407 (2001).
[5] T. Nikuni, M. Oshikawa, A. Oosawa, and H. Tanaka, Phys. Rev. Lett. **84**, 5868 (2000).
[6] Ch. Rüegg, N. Cavadini, A. Furrer, H.-U. Güdel, K. Krämer, H. Mutka, A. Wildes, K. Habicht, and P. Vorderwisch, Nature (London) **423**, 62 (2003).
[7] M. P. A. Fisher, P. B. Weichman, G. Grinstein, and D. S. Fisher, Phys. Rev. B **40**, 546 (1989).
[8] T. Giamarchi, Ch. Rüegg, and O. Tchernyshyov, Nat. Phys. **4**, 198 (2008).
[9] R. Yu, L. Yin, N. S. Sullivan, J. S. Xia, Ch. Huan, A. Paduan-Filho, N. F. Oliveira, Jr., S. Haas, A. Steppke, C. F. Miclea, F. Weickert, R. Movshovich, E.-D. Mun, B. L. Scott, V. S. Zapf, and T. Roscilde, Nature (London) **489**, 379 (2012).
[10] A. Zheludev, Z. Honda, Y. Chen, C. L. Broholm, K. Katsumata, and S. M. Shapiro, Phys. Rev. Lett. **88**, 077206 (2002).
[11] Y. Maeda, Ch. Hotta, and M. Oshikawa, Phys. Rev. Lett. **99**, 057205 (2007).
[12] S. A. Zvyagin, J. Wosnitza, C. D. Batista, M. Tsukamoto, N. Kawashima, J. Krzystek, V. S. Zapf, M. Jaime, N. F. Oliveira, Jr., and A. Paduan-Filho, Phys. Rev. Lett. **98**, 047205 (2007).
[13] H. Manaka, A. V. Kolomiets, and T. Goto, Phys. Rev. Lett. **101**, 077204 (2008).
[14] H. Manaka, H. A. Katori, O. V. Kolomiets, and T. Goto, Phys. Rev. B **79**, 092401 (2009).
[15] F. D. M. Haldane, Phys. Rev. Lett. **50**, 1153 (1983).
[16] T. Hong, A. Zheludev, H. Manaka, and L.-P. Regnault, Phys. Rev. B **81**, 060410 (2010).

[17] T. Roscilde, Phys. Rev. B **74**, 144418 (2006).
[18] S. Wessel and S. Haas, Phys. Rev. B **61**, 15262 (2000).
[19] D. C. Dender, P. R. Hammar, D. H. Reich, C. Broholm, and G. Aeppli, Phys. Rev. Lett. **79**, 1750 (1997).
[20] M. Köppen, M. Lang, R. Helfrich, F. Steglich, P. Thalmeier, B. Schmidt, B. Wand, D. Pankert, H. Benner, H. Aoki, and A. Ochiai, Phys. Rev. Lett. **82**, 4548 (1999).
[21] R. Feyerherm, S. Abens, D. Günther, T. Ishida, M. Meiner, M. Meschke, T. Nogami, and M. Steiner, J. Phys.: Condens. Matter **12**, 8495 (2000).
[22] B. Schmidt, H. Aoki, T. Cichorek, J. Custers, P. Gegenwart, M. Kohgi, M. Lang, C. Langhammer, A. Ochiai, S. Paschen, F. Steglich, T. Suzuki, P. Thalmeier, B. Wand, and A. Yaresko, Physica B **300**, 121 (2001).
[23] H. Aoki, Ph.D. thesis, Tohoku University, 2000.
[24] G. Kamieniarz, W. Florek, and M. Antkowiak, Phys. Rev. B **92**, 140411(R) (2015).
[25] R. Matysiak, P. Gegenwart, A. Ochiai, M. Antkowiak, G. Kamieniarz, and F. Steglich, Phys. Rev. B **88**, 224414 (2013).
[26] R. Matysiak, G. Kamieniarz, P. Gegenwart, and A. Ochiai, Phys. Rev. B **79**, 224413 (2009).
[27] See Supplemental Material at http://link.aps.org/supplemental/10.1103/PhysRevB.94.100403 for separation of the magnetic part of the specific heat from the raw data and for the residuals calculated for the DTN compound.
[28] H. Shiba, K. Ueda, and O. Sakai, J. Phys. Soc. Jpn. **69**, 1493 (2000).
[29] N. Shibata and K. Ueda, J. Phys. Soc. Jpn. **70**, 3690 (2001).
[30] M. Oshikawa, K. Ueda, H. Aoki, A. Ochiai, and M. Kohgi, J. Phys. Soc. Jpn. **68**, 3181 (1999).
[31] K. Iwasa, M. Kohgi, A. Gukasov, J.-M. Mignot, N. Shibata, A. Ochiai, H. Aoki, and T. Suzuki, Phys. Rev. B **65**, 052408 (2002).
[32] G. Kamieniarz and R. Matysiak, Comput. Mater. Sci. **28**, 353 (2003).
[33] P. Gegenwart, H. Aoki, T. Cichorek, J. Custers, N. Harrison, M. Jaime, M. Lang, A. Ochiai, and F. Steglich, Physica B **312-313**, 315 (2002).
[34] H. Aoki, A. Ochiai, M. Oshikawa, and K. Ueda, Physica B **281-282**, 465 (2000).
[35] I. Affleck and M. Oshikawa, Phys. Rev. B **60**, 1038 (1999).
[36] E. Altman, Y. Kafri, A. Polkovnikov, and G. Refael, Phys. Rev. Lett. **100**, 170402 (2008).